33rd Annual International Conference of the IEEE EMBS
Boston, Massachusetts USA, August 30 - September 3, 2011

# Investigation of EEG and MEG Source Imaging Accuracy in Reconstructing Extended Cortical Sources

Lei Ding, *Member, IEEE,* and Han Yuan, *Student Member, IEEE*

***Abstract*—Electroencephalography (EEG) and magneto-encephalography (MEG) are both currently used to reconstruct brain activity. The performance of inverse source reconstructions is dependent on the modality of signals in use as well as inverse techniques. Here we used a recently proposed sparse source imaging technique, i.e., the variation-based sparse cortical current density (VB-SCCD) algorithm to compare the use of EEG or MEG data in reconstructing extended cortical sources. We conducted Monte Carlo simulations as comparison to two other widely used source imaging techniques. The VB-SCCD technique was further evaluated in experimental EEG and MEG data. Our present results indicate that EEG and MEG have similar reconstruction performance as indicated by a metric, the area under the receiver operating characteristic curve (AUC). Furthermore, EEG and MEG have different advantages and limitations in revealing different aspects of features of extended cortical sources, which are complimentary to each other. A simultaneous EEG and MEG analysis framework is thus promising to produce much improved source reconstructions.**

## I. Introduction

Electroencephalography (EEG) and magneto-encephalography (MEG) provide excellent temporal resolutions for studying neuronal events. Meanwhile, both EEG and MEG are currently used to reconstruct brain activity to improve the identification and localization of underlying cortical neural sources. This is achieved by the so-called electromagnetic source imaging (ESI) techniques [1] that non-invasively reconstruct cortical electrical activity from external surface potentials and/or magnetic fields, known as the EEG/MEG 'inverse problem'. While EEG and MEG signals reflect common neural electrical events, there is great interest in the assessment of the relative accuracy of EEG and MEG in reconstructing neural sources, which depends on the modality of signals as well as many other factors, including the accuracy of forward modeling and the performance of inverse reconstruction algorithms.

There have been many debates over the accuracy of EEG or MEG based source localization and/or reconstruction approaches. Due to its biophysical property, MEG is mainly limited by less sensitivity to radially oriented cortical sources [2]. Since deep brain sources are nearly radial, the sensitivity of MEG to deep sources drops rapidly [3]. On the other hand, EEG reflects current sources of all orientations. However, when field gradient distributions are concerned, the electrical field gradient can be smoothed by low skull conductivity, which makes EEG signals more vulnerable to noises than MEG signals. Furthermore, the electrical field gradient reaches the highest along the current dipole moment whereas the magnetic field has the highest gradient across the current dipole moment.

Previous studies [4], [5] have reported better localization accuracy using MEG than EEG. Other studies [6], however, indicated comparable performance of EEG and MEG. These conflicting data suggested various factors influencing the performance of EEG and MEG. Generally, in experimental studies, it is difficult to distinguish errors occurred during forward head modeling, errors caused by inverse reconstructions, and errors due to inherent differences between EEG and MEG signals. Instead, through the use of modeling studies, it is possible to examine the relative accuracy of EEG and MEG using the same forward solution to generate both synthetic external EEG/MEG measurements and inspect resulted inverse solutions.

In the present study, we conducted the Monte Carlo simulation study to compare the accuracy of EEG and MEG signals in reconstructing extended cortical sources using cortical current density (i.e., CCD) source model. We aimed to investigate the accuracy of EEG and MEG using a newly developed sparse source imaging technique, i.e., the variation-based sparse cortical current density (VB-SCCD) algorithm [7]. We further compared the performance of the sparse source imaging algorithm based on EEG/MEG data as opposed to other two L2-norm based inverse algorithms, i.e., weighted minimum norm estimate (wMNE) [8] and cortical low resolution electromagnetic tomography (cLORETA) [9]. In addition to simulations, experimental EEG and MEG data from a face recognition task [10] were used to further compare the accuracy of EEG and MEG in reconstructing realistic cortical sources.

## II. Method

### A. wMNE, cLORETA, and VB-SCCD

Assume the vector $\bar{S}$ represents $N$ elemental dipole moments defined on the CCD model. Vectors $\bar{v}$ and $\bar{b}$ denote potentials and magnetic fields measured at $M_v$ EEG electrodes and $M_b$ MEG sensors, respectively. $A_v = (\bar{a}_{v,1}, \bar{a}_{v,2}, \cdots, \bar{a}_{v,N})$ is the gain matrix $(M_v \times N)$ and each column specifies potentials on electrodes from a unity dipole, while $A_b = (\bar{a}_{b,1}, \bar{a}_{b,2}, \cdots, \bar{a}_{b,N})$ is the corresponding gain

Manuscript received April 15, 2011. This work was supported in part by OCAST HR09-125S, NSF CAREER ECCS-0955260, and DOT-FAA 10-G-008.

*L. Ding is with the School of Electrical and Computer Engineering and Center for Biomedical Engineering, University of Oklahoma, Norman, OK 73019 (phone: 4053254577; fax: 4053257066; e-mail: leiding@ou.edu).

H. Yuan is with the Laureate Institute for Brain Research, Tulsa, OK 74136 USA (e-mail: hyuan@laureateinstitute.org).

matrix $(M_b \times N)$ for magnetic fields. $\bar{n}_v$ and $\bar{n}_b$ denote background and measurement noises in EEG and MEG, respectively. Then the forward problem can be expressed in the following vector notation:

$$\bar{v} = A_v \bar{s} + \bar{n}_v \quad \text{and} \quad \bar{b} = A_b \bar{s} + \bar{n}_b \qquad (1)$$

In the following formulation of inverse problems, symbols for electrical potentials and magnetic fields are not distinguished for the simplicity. We use $\bar{\phi}$ to denote observations resulted from either electrical potentials or magnetic fields and use $A$ to denote the corresponding gain matrix from either signal modality. The regularization scheme used in the wMNE inverse algorithm can be stated as the following optimization problem.

$$\min \left\| W\bar{s} \right\|_2 \qquad subject \quad to \quad \left\| \bar{\phi} - A\bar{s} \right\|_2 < \beta \qquad (2)$$

where $\beta$ is the regularization parameter. $W$ is an $N \times N$ diagonal matrix and its diagonal element is calculated by $W_{ii} = \sqrt{A_i^T A_i}$, which is used to compensate the bias due to the source depth [8].

The optimization problem in the cLORETA algorithm [9] can be stated as

$$\min \left\| LW\bar{s} \right\|_2 \qquad subject \quad to \quad \left\| \bar{\phi} - A\bar{s} \right\|_2 < \beta \qquad (3)$$

where $L$ is the two-dimensional discrete spatial Laplacian operator defined over the cortical surface. The penalty term here is to minimize the contribution from high spatial frequency components and, thus cLORETA usually provides smooth source reconstructions.

The regularization schemed used in VB-SCCD algorithm is developed based on the theory of sparse source imaging [11]. The optimization problem proposed to be solved in VB-SCCD can be mathematically stated as

$$\min \left\| V\bar{s} \right\|_1 \qquad subject \quad to \quad \left\| \bar{\phi} - A\bar{s} \right\|_2 < \beta \qquad (4)$$

where $V$ is a matrix operator to get the variation map of cortical current density distributions. The variation vector is thus defined as $V\bar{s}$. The penalty function is designed to minimize the L1-norm of variation vector of solution, which is equivalent to maximize the sparseness in the variation domain. Each element in this variation vector represents a coefficient within the variation map over a triangular edge in the CCD model and its value indicates the current density difference between two triangular elements sharing the same edge (see [7] for details).

Equations (2), (3), and (4) are solved by the second-order cone programming [12]. The regularization parameter $\beta$ in equations (2), (3), and (4) can be estimated by applying the discrepancy principle [13]. We choose it to be high enough so that the probability of $\left\| \bar{n} \right\|_2 \geq \beta$, where $\bar{n} = \bar{\phi} - A\bar{s}$, is small. When noise is Gaussian white, $(1/\sigma^2)\left\| \bar{n} \right\|_2^2$, where $\sigma^2$ denotes the variance, has the $\chi_m$ distribution with $M$ degrees of freedom, i.e. $(1/\sigma^2)\left\| \bar{n} \right\|_2^2 \sim \chi_m^2$. In practice, the upper bound of $\left\| \bar{n} \right\|_2$, i.e. $\beta$, is selected such that the confidence interval $[0, \beta]$ integrates to a 0.99 probability [11]. In conditions with real noise, other noise models can be similarly utilized if the distributions of noise are known or can be estimated.

### B. Monte Carlo Simulation Protocol

Since the majority of EEG and MEG signals are generated by cortical pyramidal neurons [14], the cortical current density (CCD) source model [15] was used in the present study. A current dipole was used to model current source at each elemental triangle on the CCD model and its orientation was set in the normal direction of the triangle. The CCD model used in simulation was generated by the BrainSuite software [16], which segmented the interface between white matter and gray matter from a human head magnetic resonance imaging (MRI) data. The volume conduction was modeled by a three-shell boundary element model (BEM) with three major tissues (the scalp, skull, and brain) of different conductivity (0.33/Ω.m, 0.0165/Ω.m, and 0.33/Ω.m, respectively) [17]. EEG electrode locations and MEG sensor locations and orientations were adapted from the realistic EEG and MEG systems. For EEG, 120 channels were selected from a realistic 128-electrodes EGI system (Electrical Geodesics, Inc., Eugene, OR) by removing face electrodes. For MEG, there were 151 MEG sensors from a 151 channel CTF Omega system.

Extended cortical sources were generated by selecting a seed triangle on the CCD model and gradually growing into patches by iteratively adding neighboring triangles. The dipole moment on each triangle was computed as the multiplication of the individual triangular area and the dipole moment density (assume 100 pAm/mm$^2$). Single-source and two-source conditions were simulated and the locations of simulated sources were randomly selected (i.e., 200 locations). The cortical extents of these sources were between 2 cm$^2$ to 4 cm$^2$. We used the metrics, i.e., the receiver operating characteristic (ROC) curve and the area under the ROC curve (AUC) from the detection theory (see [7] for details) to evaluate the performance of wMNE, cLORETA, and VB-SCCD.

### C. Experimental Data Protocol

We also performed the analysis of EEG and MEG data from a face recognition task [10] from a subject. Details of the experimental paradigm as well as the full dataset can be found at www.fil.ion.ac.ik/spm/data/mmfaces.html. In this experiment, the subject made symmetry judgments on faces and scrambled faces, which were presented every 3.6 s and each stimulus lasted for 0.6 s. EEG data were acquired on a 128-channel ActiveTwo system, sampled at 2,048 Hz, while MEG data were sampled at 625 Hz from a 151-channel CTF Omega system. Epochs were created from -200 ms to 600 ms for both EEG and MEG and then averaged according to faces trials and scrambled faces trial to produce event-related data. The subject's T1-weighted MRI was obtained from a 1.5T Siemens Sonata via an MDEFT sequence with voxels in 1x1x1 mm$^3$ resolution, using a whole body coil for RF transmission and an 8-element phased array head coil for signal reception. The CCD source model and BEM volume conductor were built using the BrainSuite software. The geometry registration was performed among subject's head

shape, EEG electrode locations, and MEG sensors using a surface-fitting algorithm [18].

## III. Results

Fig. 1 shows the AUC values for simulations from all different conditions. To compare the use of EEG and MEG data, sources estimations were based on EEG and MEG data computed via the same forward model. In the case of a single simulated source (Fig. 1(a)), the median AUC values achieved by VB-SCCD were 0.8753 and 0.8502 for the EEG and MEG data, respectively. Although on average EEG produces slightly higher AUC values than MEG, they are not statistically significant ($p$ > 0.05). The close performance of EEG and MEG data is also observed in the case of two-source conditions (Fig. 1(b)), while the AUC values of two-source data are lower than that of the single-source condition. To further evaluate the use of EEG/MEG data, their AUC values achieved by VB-SCCD were also compared as opposed to wMNE and cLORETA. For both wMNE and cLORETA, the difference in terms of AUC values between EEG data and MEG data is statistically significant ($p$ < 0.05) for both single- and two-source conditions, while such a difference is more evident in wMNE. Furthermore, the performance of VB-SCCD in reconstructing extended cortical sources using either EEG or MEG data is significantly better than wMNE and cLORETA (all $p$ <0.05).

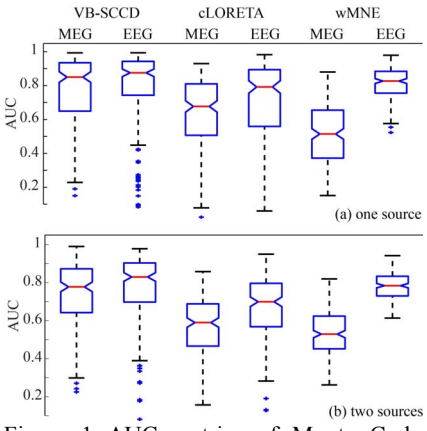


Figure 1 AUC metrics of Monte Carlo simulations (Whisker plots) for different signal modality (i.e., EEG and MEG), different methods (i.e., VB-SCCD, wMNE, and cLORTEA), and different number of sources (i.e., 1 (a) and 2 (b)).

The factors contributing to an AUC metric include the error in identifying source locations and the error in estimating source extents. In the next step, we examined the representative examples of reconstructed sources from both EEG and MEG to see whether there are different reasons causing the decrease of AUC values using both types of signals. Fig. 2 shows the two examples with one having the best AUC value from EEG (Fig. 2(a)) and one having the best AUC value from MEG (Fig. 2(b)) using the VB-SCCD algorithm. Their corresponding MEG and EEG reconstruction results are also displayed. As illustrated in Fig. 2(a), when using EEG data two sources were correctly localized and their spatial extents were well reconstructed, resulting in the highest AUC value (i.e., 0.9781). In contrast, under the same simulation condition, one source was missing in MEG, which yielded a lower AUC value. In another case of two-source simulation illustrated in Fig 2(b), the accuracy for localization and extent estimation are both high for the two sources, which leads to the highest AUC value (i.e., 0.9901) using MEG data. On the contrary, in this case, while sources reconstructed using EEG data are localized to the correct places, their spatial extents are smeared, which results in decreased AUC value. These results suggest that low AUC values with EEG are usually caused by smeared source distributions, which contributes errors for the accurate estimation of spatial extents of sources. The low AUC values with MEG are more likely to be caused by missing sources, which contributes errors in terms of localization. Both errors are reflected in the AUC metric.

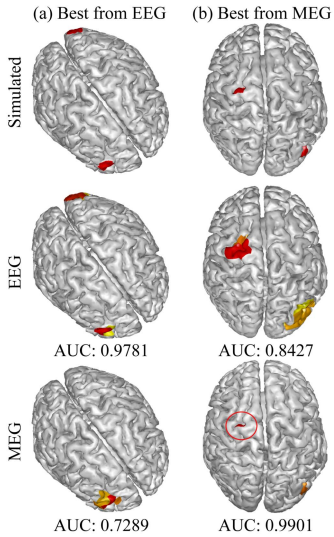


Figure 2 Visualization of two examples with the highest AUC values from EEG (a) and MEG (b), and their corresponding MEG and EEG results, obtained from VB-SCCD.

We also compared the performance of VB-SCCD in experimental EEG and MEG data. Results are shown in Fig. 3, which includes brain sources from face trials during both P100/M100 and N170/M170 components. Reconstructed sources from EEG and MEG are generally consistent with each other. Bilateral activity within the visual cortex can be observed at P100/M100 using either EEG or MEG data. Fusiform activations during N170/M170 appear unilaterally dominant using either EEG or MEG. Meanwhile, EEG results reveal some activity within the frontal cortex (e.g., 150 ms), which is also expected in face recognition [10]. Sources reconstructed from MEG seem much more localized compared with sources reconstructed from EEG (e.g., 120 ms), which is consistent with our observation in simulations (Fig. 2).

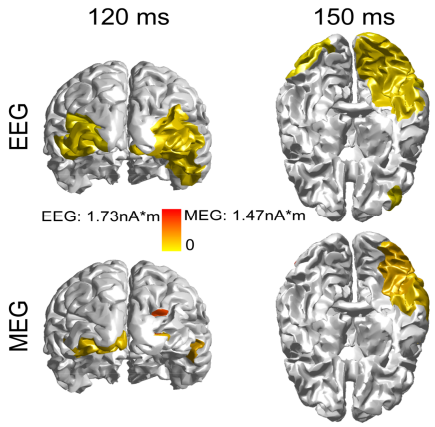


Figure 3 Comparison between EEG and MEG using VB-SCCD in reconstructing sources behind P100/M100 and P170/M170.

## IV. Discussions

In the present study, we conducted a Monte Carlo simulation study to compare the performance of EEG and MEG in reconstructing extended cortical sources using a newly developed sparse source imaging technique (i.e., VB-SCCD) [7]. We also compared the performance of EEG and MEG in the same simulation protocol using other two widely reported L2-norm source imaging techniques (i.e. wMNE and cLORETA). From our simulation data, results indicate that EEG and MEG have similar performance in localizing extended cortical sources as well as reconstructing their spatial extents by the VB-SCCD inverse imaging technique, as evaluated by the metric AUC [19]. Such difference between EEG and MEG becomes large and statistically significant in other two techniques (i.e., wMNE and cLORETA), which suggests that the use of information in different inverse algorithms from EEG and MEG might varies. Our findings of the modality-dependent and algorithm-dependent performance in source reconstruction corroborate the controversial reports in literature [4]-[6] about the use of EEG and MEG. Thus the accuracy of EEG and MEG data for inverse source imaging depends on factors beyond signal characteristics, such as specific inverse methods used as well as forward models and signal-noise ratios (which are not investigated in the current study). Among the three techniques investigated in the present study, the VB-SCCD technique not only has the significantly better reconstruction accuracy for extended cortical sources than other two techniques, but also produces comparable results using EEG and MEG.

By directly visualizing sources reconstructed by VB-SCCD using EEG and MEG, it further reveals the complimentary features of EEG and MEG in reconstructing cortical sources. MEG tends to produce focused sources which are consistent with simulated sources in terms of spatial extent, while EEG tends to smear spatial distributions of sources (Fig. 2) which might be caused by the relatively low EEG field gradients as compared to MEG field gradients as discussed in the Introduction section. On the other hand, MEG tends to produce missing cortical sources (Fig. 2), which can be explained by its degraded sensitivity to radial sources [2]. The simultaneous use of both EEG and MEG that integrates their complementary features will be a promising option to resolve these problems [20].

We further evaluated the performance difference of EEG and MEG using VB-SCCD using experimental data from a face recognition task. The cortical sources reconstructed for visual response (i.e., P100/M100) and face recognition (P170/M170) indicate the same difference pattern between EEG and MEG as from simulations. MEG results missed the sources from frontal cortex, while EEG results show much smeared source distributions in both visual cortex and fusiform areas.

In summary, the performance of EEG and MEG data in reconstructing extended cortical sources is shown to be dependent on the inverse techniques used. Furthermore, both EEG and MEG have different advantages and limitations in revealing different aspects of features of extended cortical sources. A simultaneous data analysis framework integrating both EEG and MEG data is expected to produce improved performance for cortical source reconstruction.

## References


[1] R. Grech, T. Cassar, J. Muscat, K. P. Camilleri, S.G. Fabri, M. Zervakis, P. Xanthopoulos, V. Sakkalis, and B. Vanrumste, "Review on solving the inverse problem in EEG source analysis," *Journal of Neuroengineering and Rehabilitation,* vol. 5, pp. 5-25, 2008.

[2] G. Baule, and R. McFee, "Theory of magnetic detection of the heart's electrical activity," *J Appl Phys*, vol. 36, pp. 2066–2073, 1965.

[3] F.H. Lin, J. W. Belliveau, A.M. Dale, and M.S. Hämäläinen, "Distributed Current Estimates Using Cortical Orientation Constraints," *Hum Brain Mapp,* vol. 27, pp. 1-13, 2006.

[4] S. Gharib, W.W. Sutherling, N. Nakasato, D.S. Barth, C. Baumgartner, N. Alexopoulos, S. Taylor, and R.L. Rogers, "MEG and ECoG localization accuracy test," *Electroencephalogr Clin Neurophysiol,* vol. 94, pp. 109–114, 1995.

[5] T. Yamamoto, S.J. Williamson, L. Kaufman, C. Nicholson, and R. Llinas, "Magnetic localization of neuronal activity in the human brain," *Proc Natl Acad Sci USA*, vol. 85, pp. 8732–8736, 1988.

[6] T. Krings, K.H. Chiappa, B.N. Cuffin, B.R. Buchbinder, and G.R. Cosgrove, "Accuracy of electroencephalographic dipole localization of epileptiform activities associated with focal brain lesions," *Ann. Neurol.*, vol. 44, pp. 76–86, 1998.

[7] L. Ding, "Reconstructing Cortical Current Density by Exploring Sparseness in the Transform Domain," *Physics in Medicine and Biology*, vol. 54, pp. 2683-2697, 2009.

[8] B. Jeffs, R. Leahy, and M. Singh, "An evaluation of methods for neuromagnetic image reconstruction," *IEEE Trans. Biomed. Eng.,* vol. 34, pp. 713-723, 1987.

[9] M. Wagner, M. Fuchs, H.A. Wischmann, R. Drenckhahn, and T. Köhler, "Smooth reconstruction of cortical sources from EEG or MEG recordings," *NeuroImage,* vol. 3, pp. S168, 1996.

[10] R.N. Henson, Y. Goshen-Gottstein, T. Ganel, L.J. Otten, A. Quayle, and M.D. Rugg, "Electrophysiological and Haemodynamic Correlates of Face Perception, Recognition and Priming," *Cerebral Cortex,* vol. 13, pp. 793-805, 2003.

[11] L. Ding and B. He, "Sparse source imaging in EEG with accurate field modeling," *Human brain mapping*, vol. 29, pp. 1053-1067, 2008.

[12] A. Nemirovski and A. Ben Tal, *Lectures on Modern Convex Optimization. Analysis*, Algorithms and Engineering Application, SIAM, 2001.

[13] A.V. Morozov, "On the solution of functional equations by the method of regularization," *Soviet. Math. Dokl.*, vol. 7, pp. 414-417, 1966.

[14] Nunez PL, 1981. *Electric field of the brain*. London: Oxford University Press.

[15] A.M. Dale and M.I. Sereno, "Improved localization of cortical activity by combining EEG and MEG with MRI cortical surface reconstruction: a linear approach," *J. Cog. Neurosci.,* vol. 5, pp. 162-176, 1993.

[16] D.W. Shattuck and R.M. Leahy, "BrainSuite: an automated cortical surface identification tool," *Med. Image Anal.,* vol. 6(2), pp. 129-142, 2002.

[17] Y. Lai, W. van Drongelen, L. Ding, K. Hecox, V.L. Towle, D.M. Frim and B. He, "Estimation of in vivo human brain-to-skull conductivity ratio from simultaneous extra- and intra-cranial electrical potential recordings," *Clinical Neurophysiology*, vol. 116, pp. 456-465, 2005.

[18] V.L. Towle, L. Khorasani, S. Uftring, C. Pelizzari, R.K. Erickson, J.P. Spire, K. Hoffmann, D. Chu and M. Scherg, "Noninvasive identification of human central sulcus: a comparison of gyral morphology, functional MRI, dipole localization, and direct cortical mapping," *NeuroImage*, vol. 19, pp. 684-697, 2003.

[19] C. Grova, J. Daunizeau, J.M. Lina, C.G. Benar, H. Benali, J. Gotman, "Evaluation of EEG localization methods using realistic simulations of interictal spikes," *NeuroImage,* vol. 29, pp. 734-753, 2006.

[20] A. Molins, S. Stufflebeam, E. Brown and M.S. Hämäläinen, "Quantification of the benefit from integrating MEG and EEG in minimum L2-norm estimation," *NeuroImage*, vol. 42, pp. 1069-1077, 2008.